

SPATIAL MODEL OF RUNOFF FLOWING INTO THE NEWLY FORMED LAKE AT SINABUNG VOLCANO

Sandy Budi WIBOWO¹, **Polin Mouna TOGATOROP^{2,3}**, **Tsamara HANINDHIYA⁴**,
Barandi Sapta WIDARTONO¹, **R. Ibnu ROSYADI¹**

DOI: 10.21163/GT_2023.182.05

ABSTRACT:

Volcanic dams are formed when eruptions occur near rivers, obstructing the natural flow of water and creating a dam. The infrequent nature of volcanic dams has resulted in limited research and literature on this topic. However, the Sinabung stratovolcano offers a valuable opportunity to address these knowledge gaps. Over a span of ten years of eruptions, abundant volcanic materials have accumulated in the Lau Borus River, leading to the growth of a dam and the formation of a lake behind it. This research aims to develop a GIS model that simulates the runoff flowing into the newly formed lake at Sinabung volcano. The methodology employed in this study involves the integration of an Agent-Based Model and Geographic Information System to create a dynamic model of runoff and spatio-temporal mapping. The results indicate that raindrops transform into runoff, flowing down the eastern volcanic flank towards the lake, covering a distance of 3.7 km from the crater in 696 seconds, with an average flow velocity of 5.32 m/s. The runoff accumulates in three drainage networks and exhibits two flow pulsations. By combining the Agent-Based Model and Geographic Information System, the research successfully identifies the process of runoff accumulation into the newly formed lake at Sinabung volcano. Further investigation into potential lake outburst scenarios would be crucial for developing comprehensive mitigation strategies for cascading volcanic disasters.

Key-words: *Sinabung volcano, runoff, Agent Based Model, GIS, lahars, disasters.*

1. INTRODUCTION

Sinabung volcano (2,460 m) had been classified as dormant volcano by Vulcanological Survey of Indonesia until it surprisingly erupted in 2010. The eruption still continues in 2021 and produces abundant pyroclastic materials at eastern and southern flank after 11 years. Tropical climate regime in Indonesia accelerates the initiation of rain-triggered lahars at Sinabung volcano. Since the year 2010, the Lau Borus River channel has experienced noteworthy transformations in its physical characteristics. These alterations can be attributed to the occurrence of multiple massive lahars, which have been responsible for transporting significant quantities of sands, gravels, and boulders along the river. As a result of these lahars, the morphology of the river channel has been reshaped, leading to the formation of a new lake. The process by which this new lake has emerged bears resemblance to the formation of landslide dams in mountainous regions. In both cases, natural forces cause the accumulation of materials, such as sediments and debris, which obstruct the normal flow of water. This obstruction ultimately results in the creation of a lake or reservoir. Similarly, in the context of the Lau Borus River channel, the lahars have contributed to the buildup of materials that have acted as a barrier, leading to the formation of the new lake. The formation of this lake signifies a significant change in the local landscape and hydrological dynamics. It highlights the impact of lahars on the natural environment and serves as an example of the complex interactions between geological processes and the formation of landforms.

¹Department of Geographic Information Science, Faculty of Geography, Universitas Gadjah Mada, Indonesia; sandy_budi_wibowo@ugm.ac.id; barandi@geo.ugm.ac.id; ibnurosyadi@gmail.com)

²Ministry of Agrarian Affairs and Spatial Planning / National Land Agency, Indonesia, polin.mtogatorop@atrbpn.go.id

³Master of Science in Remote Sensing Study Program, Faculty of Geography, Universitas Gadjah Mada, Indonesia, polinmouna@mail.ugm.ac.id

⁴Cartography and Remote Sensing Study Program, Faculty of Geography, Universitas Gadjah Mada, Indonesia, tsamarahanindhiya@mail.ugm.ac.id

The existence of this newly formed lake is challenging because like other landslide dams in the world, there is possibility of failure. It could produce voluminous volcanic debris flows causing fatal and devastating impacts at downstream area. The objective of this study is to develop spatial model of runoff flowing into new formed lake at Sinabung volcano. This would be important to estimate the evolution of water volume and to support disaster mitigation strategies due to dam failure at the outlet.

2. LITERATURE REVIEW

North Sumatra is very well known worldwide for the Toba caldera, which resulted from the eruption of a supervolcano (Chesner et al., 2020; Mukhopadhyay et al., 2022; Naen et al., 2023). A dormant stratovolcano volcano is located at ignimbrite plateau 34 km north from this caldera, named Sinabung (Fig. 1).

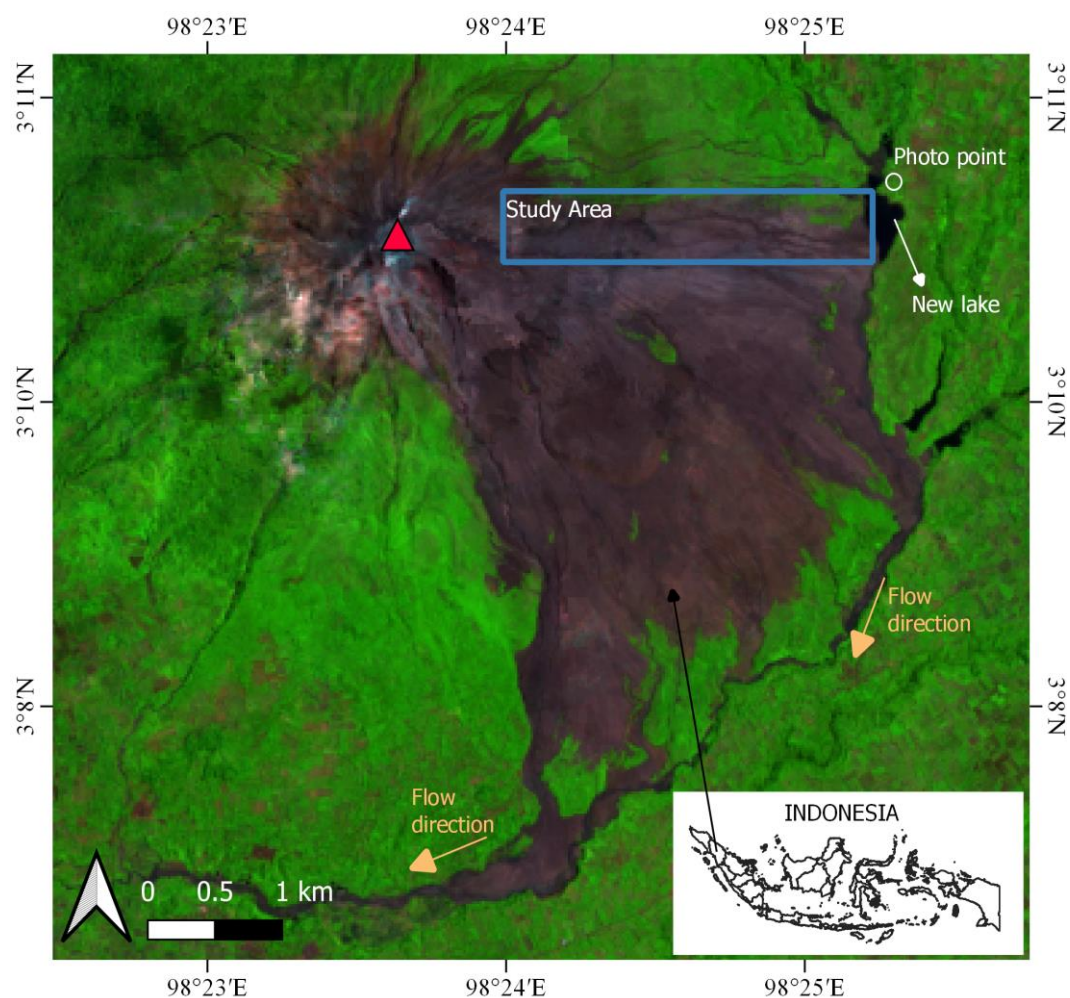


Fig. 1. Sentinel 2 satellite imagery (SWIR composite B12, B8A, B4) in 2020 showing the study area at the eastern flank of Sinabung volcano. New lake was formed due to excessive lahar deposition in Lau Borus River.

Unlike Toba caldera, Sinabung volcano was not famous at that time because there were no records on its volcanic activity since 1600. Then, its phreatic eruption in 2010 surprised Indonesian people, scientists, and volcanologists. The volcanic activity has undergone a transformation, shifting towards the formation and destruction of lava domes. This process has persisted for over ten years.

Consequently, the volcanoes have released an amount exceeding 0.16 km³ of pyroclastic materials (Nakada et al., 2019) over an area of approximately 25.5 km² (Kadavi et al., 2017). The last pre-historic eruption produced lava flows, deposit of Pyroclastic Density Currents (PDC) and lahars as well, without evidence of pumice-fall sedimentation. This indicates that this stratovolcano never had explosive/plinian eruption and it doesn't change until now. Most of the pyroclastic materials (basaltic andesite to andesite) are deposited 4.5 km from the summit. Some studies have been conducted at this volcano including photogrammetry (Carr et al., 2019), GPS observation (Hotta et al., 2019); tectonic activity (Kriswati et al., 2019), and tomography (Indrastuti et al., 2019).

Drainage pattern of this stratovolcano is classified as radial, where many tributaries radiate outward from summit (Supriyati and Tjahjono, 2018). At the downstream area, Lau Borus river channel connects these tributaries from north-eastern to south-western flank. It means that even if pyroclastic materials that transforms into lahars are eroded and transported through different tributaries and they still end up in the same main river channel (Lau Borus). Hence, this particular river has the capability to accumulate and transport significant amounts of materials (more than 0.16 km³ spread over 25.5 km²) through a single channel that ranges in width from 51.9 to 156.56 m (Adriani and Nurwihastuti, 2017). This leads to formation of a new temporary lake of 5 ha in 2017. The area of lake is increasing in 2021 (9.84 ha). **Fig. 2** shows the picture of this lake taken from photo point that is mentioned in **Fig. 1**.

The formation of this new lake is probably similar to the mechanism of landslide dam in mountainous regions (Zhong et al., 2021; Takayama et al., 2021; Sun et al., 2021). Earth materials coming from riverbank block the river and hold the water flow at the upstream part. The dimensions of landslide dams are predominantly determined by the topographical characteristics of the nearby hills and the morphometric attributes of the rivers. Serious consequences could happen in case of overtopping, breaching or dam failure (Zhong et al., 2020; Yang et al., 2020; Ruan et al., 2021; Tsai et al., 2021). Thus, detailed evaluation of these temporal dams is needed in order to support structural and non-structural mitigation strategies.

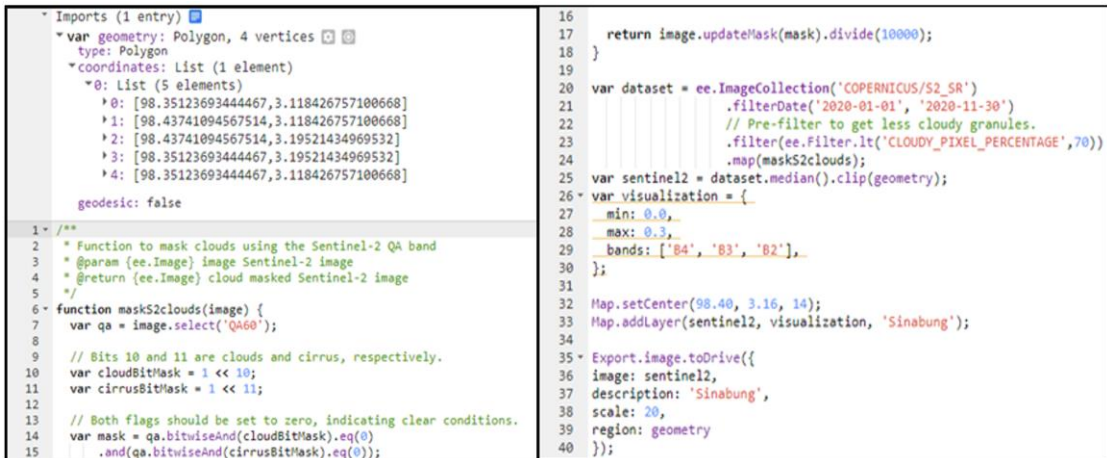


Fig. 2. Panoramic photo of a new lake formed in Lau Borus River channel.

Coupling between Agent Based Model (ABM) and Geographic Information System (GIS) allow to perform dynamic model. This is important to predict the quantity of runoff flowing into newly formed lake at Sinabung volcano. Agent Based Model focused on individual behavior in a complex environment (Abebe et al., 2019; Zhuo and Han, 2020; Aerts, 2020; Haer et al., 2020). In most of studies, agent is defined as human, vehicle, or animal who is facing a specific phenomenon. However, water, runoff or raindrop can also act as agent which respond the surrounding environment. GIS package is integrated in the ABM, so that any movement of agents still contains geographic coordinate.

3. DATA AND METHODS

This study was conducted at the eastern flank of Sinabung volcano (**Fig. 1**). The study area is located in Karo Regency, North Sumatra, Indonesia. The study area includes volcanic cone and new lake within Lau Borus River channel. Sentinel 2 satellite imagery in 2020 was used to map the area rapidly. However, clouds and cirrus had to be masked in order to get seamless imagery. The code to perform this procedure in Google Earth Engine is shown in **Fig. 3**.



```

Imports (1 entry)
var geometry: Polygon, 4 vertices
  type: Polygon
  coordinates: List (1 element)
    0: List (5 elements)
      0: [98.3512369344467, 3.118426757100668]
      1: [98.43741894567514, 3.118426757100668]
      2: [98.43741894567514, 3.19521434969532]
      3: [98.3512369344467, 3.19521434969532]
      4: [98.3512369344467, 3.118426757100668]
  geodesic: false

1 /**
2  * Function to mask clouds using the Sentinel-2 QA band
3  * @param (ee.Image) image Sentinel-2 image
4  * @return (ee.Image) cloud masked Sentinel-2 image
5  */
6 function maskS2clouds(image) {
7   var qa = image.select('QA60');
8
9   // Bits 10 and 11 are clouds and cirrus, respectively.
10  var cloudBitMask = 1 << 10;
11  var cirrusBitMask = 1 << 11;
12
13  // Both flags should be set to zero, indicating clear conditions.
14  var mask = qa.bitwiseAnd(cloudBitMask).eq(0)
15  .and(qa.bitwiseAnd(cirrusBitMask).eq(0));
16
17  return image.updateMask(mask).divide(10000);
18 }
19
20 var dataset = ee.ImageCollection('COPERNICUS/S2_SR')
21   .filterDate('2020-01-01', '2020-11-30')
22   // Pre-filter to get less cloudy granules.
23   .filter(ee.Filter.lt('CLOUDY_PIXEL_PERCENTAGE', 70))
24   .map(maskS2clouds);
25 var sentinel2 = dataset.median().clip(geometry);
26 var visualization = {
27   min: 0.0,
28   max: 0.3,
29   bands: ['B4', 'B3', 'B2'],
30 };
31
32 Map.setCenter(98.40, 3.16, 14);
33 Map.addLayer(sentinel2, visualization, 'Sinabung');
34
35 Export.image.toDrive({
36 image: sentinel2,
37 description: 'Sinabung',
38 scale: 20,
39 region: geometry
40 });

```

Fig. 3. Code for cloud masking of Sentinel 2 Imageries in Google Earth Engine.

This code was used to mask clouds in Sentinel-2 satellite images and display the resulting cloud-free composite image on a map. The code consists of two main parts: a function called `maskS2clouds` and the main script that uses this function. The `maskS2clouds` function takes an input Sentinel-2 image and applies a cloud mask to it. First of all, the function receives an input image as a parameter (`image`). It selects the Quality Assessment (QA) band from the input image using the `select` method and assigns it to the variable `qa`. The QA band contains information about different pixel attributes, including cloud and cirrus information. The cloud and cirrus bits are identified in the QA band. The variable `cloudBitMask` represents the bit for clouds, and `cirrusBitMask` represents the bit for cirrus. The `mask` variable is created by performing bitwise operations on the QA band. It checks if the cloud and cirrus bits are equal to zero, indicating clear conditions. The `bitwiseAnd` method is used to perform a bitwise AND operation between the QA band and the respective bit masks. The `eq` method is used to compare the result with zero, creating a binary mask. Finally, the function applies the mask to the input image using the `updateMask` method and divides the image by 10000 to scale the pixel values. The resulting masked image is returned.

After defining the `maskS2clouds` function, the main script was developed. An Image Collection from the COPERNICUS/S2_SR dataset is created using `ee.ImageCollection('COPERNICUS/S2_SR')`. The collection is filtered to include images within a specific date range using the `filterDate` method from January to November 2020. A pre-filter is applied to the collection to further filter out images with a cloudy pixel percentage greater than 60% using the `filter` method with the `ee.Filter.lt` function. The `maskS2clouds` function is mapped over the Image Collection using the `map` method. This applies the cloud mask to each image in the collection. A visualization parameter object named `visualization` is created, specifying the minimum and maximum values for visualization (`min` and `max`) and the bands to display (`bands`). The center of the map is set using the `Map.setCenter` method, providing the longitude, latitude, and zoom level of the study area. The resulting cloud-free composite image, computed and added to the map using the `Map.addLayer` method. The visualization parameter object (`visualization`) is provided to specify how the image should be displayed, and a name (`Sinabung`) is given to the layer.

The highest quality topography data available for remote area such as Sinabung volcano is DEMNAS. The Indonesia National Digital Elevation Model (DEMNAS) is constructed using several SAR imageries, such as IFSAR data with a resolution of 5m, TERRASAR-X data that has been resampled to 5m resolution from its original 5-10m resolution, and ALOS PALSAR data resampled to 5m resolution from its initial 11.25m resolution. The resampling process involves the widespread utilization of Mass Point data from the Indonesian Topography Map (Rupabumi Indonesia or RBI). DEMNAS has a spatial resolution of 0.27 arc-seconds and employs the EGM2008 vertical datum and Geotiff 32-bit float data format. For validation and accuracy of DEM, measurement of Ground Control Point (GCP) and the Geodetic Control Network (JKG) are applied (Ville et al., 2015; Wibowo and Nurani 2019; Wibowo et al., 2021; Gomez et al., 2023). The validation outcomes in Sumatra indicate that DEMNAS exhibits superior accuracy compared to high-resolution data models created using mass points, spot heights, and breaklines (referred to as DTM). The DEMNAS for the Sumatra region display Root Mean Square Errors (RMSE) of 2.79 m with bias errors of -0.13 m (Badan Informasi Geospasial, 2018).

This topography data is very important because it provides environment for agents. The code of Agent Based Model was written in NetLogo, a multi-agent programming language commonly used for simulating complex systems. It requires the NetLogo extension (GIS) and defines three global variables: `elevation`, `slope`, and `aspect`. These variables will be used to store data related to the elevation, slope, and aspect of the terrain. The `setup` procedure is responsible for initializing the simulation environment. First of all, the current state of the simulation should be cleared from any potential bugs using the function `clear-all`. The current directory should be set to load the DEM in ASCII format and assigned to the `elevation` variable. The world envelope is also set based on the envelope of the `elevation` dataset. Furthermore, the functions `set slope gis:create-raster` and `set aspect gis:create-raster` create two new raster datasets named consecutively `slope` and `aspect` with the same dimensions and envelope as the previous `elevation` dataset. A convolution operation on the `elevation` dataset is performed using a 3x3 kernel to produce the `gradient` variables. The purpose of applying the convolution operation is to compute the gradient of the elevation in both horizontal and vertical directions. Afterward, this simulation calculates the slope and aspect of the terrain based on the computed gradients. After finishing the `setup` procedure, the next step is the `go` procedure, which is the main code block that runs repeatedly to simulate the movement of agents (i.e., simulation loop) based on the gradient of the terrain. A tick counter is used to control the timing and sequencing of events. The simulation stops when there are no more agents remaining. This was used as fundamental of determination of the direction of agents during their downward movement.

Rainfall data was obtained from the Climate Hazards Group InfraRed Precipitation with Station data (CHIRPS) with a resolution of 0.05° (5.5 km). The annual precipitation in 2020 was 2737 mm/year, which is typical for a tropical climate (Wibowo, 2010). Lahars were generated when the precipitation exceeded 15 mm/day, indicating excessive runoff. For example, this occurred on 22 April, 22 August, 2 September, 8-9 September, and 3 November 2020. Spatial distribution of overland flow points was set as agent in this model. We performed more than 60,000 overland flow points which were randomly distributed at the very beginning of this simulation. The movement of these raindrops followed the slope and the aspect of the eastern flank of Sinabung volcano. The limitation of this study is that it is impossible to install field instrumentation (i.e., water level logger, load cell, automated video, geophone) to monitor runoff (Wibowo et al., 2015). Due to the highly volcanic activity producing hot pyroclastic flows toward the study area, it is strictly prohibited to conduct any activities within 5 km from the crater. The slope length along the eastern flank of this volcano, where this research was conducted, is only 3.7 km. To overcome this limitation, nine observation points were used in this simulation to replace field instrumentation. This approach allowed for the extraction of hydrographs and their comparison with the lahars hydrographs documented in the existing literature. The criteria for selecting observation points depend on the drainage network. For monitoring the main channel, observation points should be located upstream, in the middle stream, or downstream. To monitor tributaries, observation points should be placed at the confluence.

4. RESULTS AND DISCUSSIONS

Spatial model of runoff flowing into new formed lake at Sinabung volcano has been conducted in this study. DEM (9 m resolution) is employed as the environment in which each 63855 overland flow points are set up as agents. The number of agents correspond to the number of pixels, i.e. one agent per pixel. The time step unit is seconds (s). At the beginning, each agent starts to flow from their original pixel/position. However, the pattern of their movement is still unclear at time step 1 and 2. The agents begin to segregate at time step 3, even if their spatial distribution is unclear and still spread out randomly (Fig. 4).

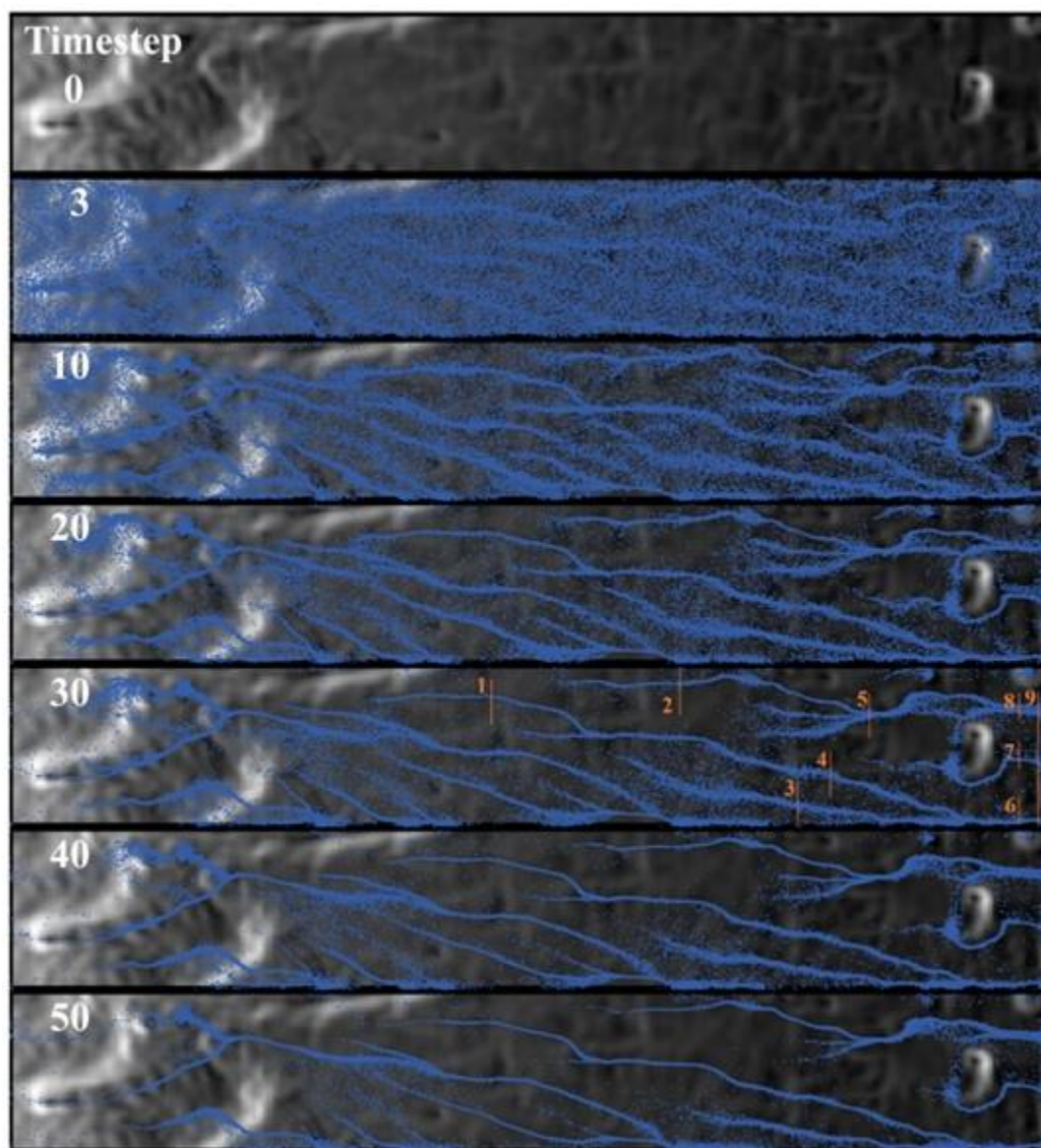


Fig. 4. Agent Based Modeling at timestep 0-50 draped over Digital Elevation Model. High and low altitude are shown by bright and dark color consecutively. The lowest altitude is the new formed lake. Hydrographs are measured at 9 observation sites.

At time step 10, the drainage pattern starts to influence the movement of agents. They are accumulated in the nearest valley. Some of agents are still on the ridge of hills, but they tend to move downward following the result of bilinear sampling between adjacent pixels of the DEM. In this Agent Based Model, the technique of bilinear sampling in GIS enables the adjustment and interpolation of pixel values between two raster grids. Its purpose is to align and harmonize the coordinates and resolutions of disparate raster datasets. The algorithm takes into account the four closest neighboring pixels to estimate the value of the desired pixel. These four pixels create a square, and their specific positions are determined by the coordinates of the target pixel. By calculating a weighted average of these neighboring pixel values, the bilinear sampling algorithm assigns a value to the target pixel. Furthermore, the pixel values within the source raster grid undergo linear changes as one moves between adjacent pixels.

At time step 20, the movement pattern of agents is clear. They follow the radial drainage pattern of the Sinabung volcanic cone. More agents are accumulated in the drainage network and they started to flow downward of the volcanic cone. At time step 30, we notice clearly the tributaries. Thus, it is easier to set up observation points in order to measure hydrograph. There are 9 observation points for each tributary which are directly connected to the lake (**Fig. 4** and **Fig. 5**). Other tributaries were not measured in detail because their estuary is located at after the lake outlet. It means that the agents do not flow to the lake direction due to the radial drainage pattern of the stratovolcano. Time step 40 is characterized by minimum number of agents that are still on the ridge. More agents are already in the tributaries compared to time step 30. While time step 50 shows total accumulation of agents within the tributaries, especially the bigger one. Smaller tributaries start losing agents since they flow downward. Time step 60 is characterized by disappearance of agents in smaller tributaries, on the contrary in bigger tributaries they accumulate and flow downstream like ordinary streamflow. Time step 70 has pretty much similar characteristic than time step 60, but the flow is steadier. This lasts until time step 100 where overland flow can only be found in bigger tributaries. After time step 100, the flow decreases gradually until time step 150. At this point, only 2 tributaries which are connected directly to the lake. The flow is still decreasing until time step 200. Time step 200 until 696 is characterized by gradual disappearance of agents at all tributaries.

Hydrogram calculated at nine observation points shows interesting pattern and also relation between upstream and downstream area. At observation point 1, there is only limited accumulation of agents from time step 0 to 50. Similar characteristics is found at observation point 2 as well. Observation point 3 which is located further downstream, has different signature. The overland flow is detected from time step 0 to 114. Overland flow at observation point 4 occurs from time step 0 to 250 with two pulsations because it is directly connected to observation 1 at upstream area. While observation point 5 which is located at the downstream part of observation 2 has an accumulation of overland flow from time step 0 to 170. The hydrograph contains two pulsations with maximum number of agents of 60. The observation point 6 is connected directly to observation 3 and 4. Its hydrogram shows an accumulation agent from time step 0 to 300 with two pulsations. Observation point 7 shares similar characteristic with observation point 1,2 and 3 since there is no other observation point at its upstream area. While observation point 8 has the same characteristic than observation point 6 since it is connected to other observation points at upstream area (2 and 5). Observation point 9 is the total accumulation of agents before they flow into the lake. Majority of the flow take place from time step 0 to 450 and it gradually diminish until time step 696.

Several lessons can be derived from the results of this study. The histogram from this model is similar and identical to that of lahars at Merapi volcano (Wibowo et al., 2015) where it involves several pulsations in it. In this study, the runoff doesn't flow more than 4 km, so that the histogram can only have 2 pulsations. At Merapi volcano, lahars can flow more than 15 km, thus it is normal to get 3-5 pulsations in a single lahar event due to its dynamic characteristics. This is caused by geological formations, topography, and drainage patterns. The topography of the Merapi stratovolcano is more complex due to the alternating formation of the old and new Merapi. It leads to meandering river channels due to the presence of Mount Kendil, located 2 km southeast of the Merapi Crater.

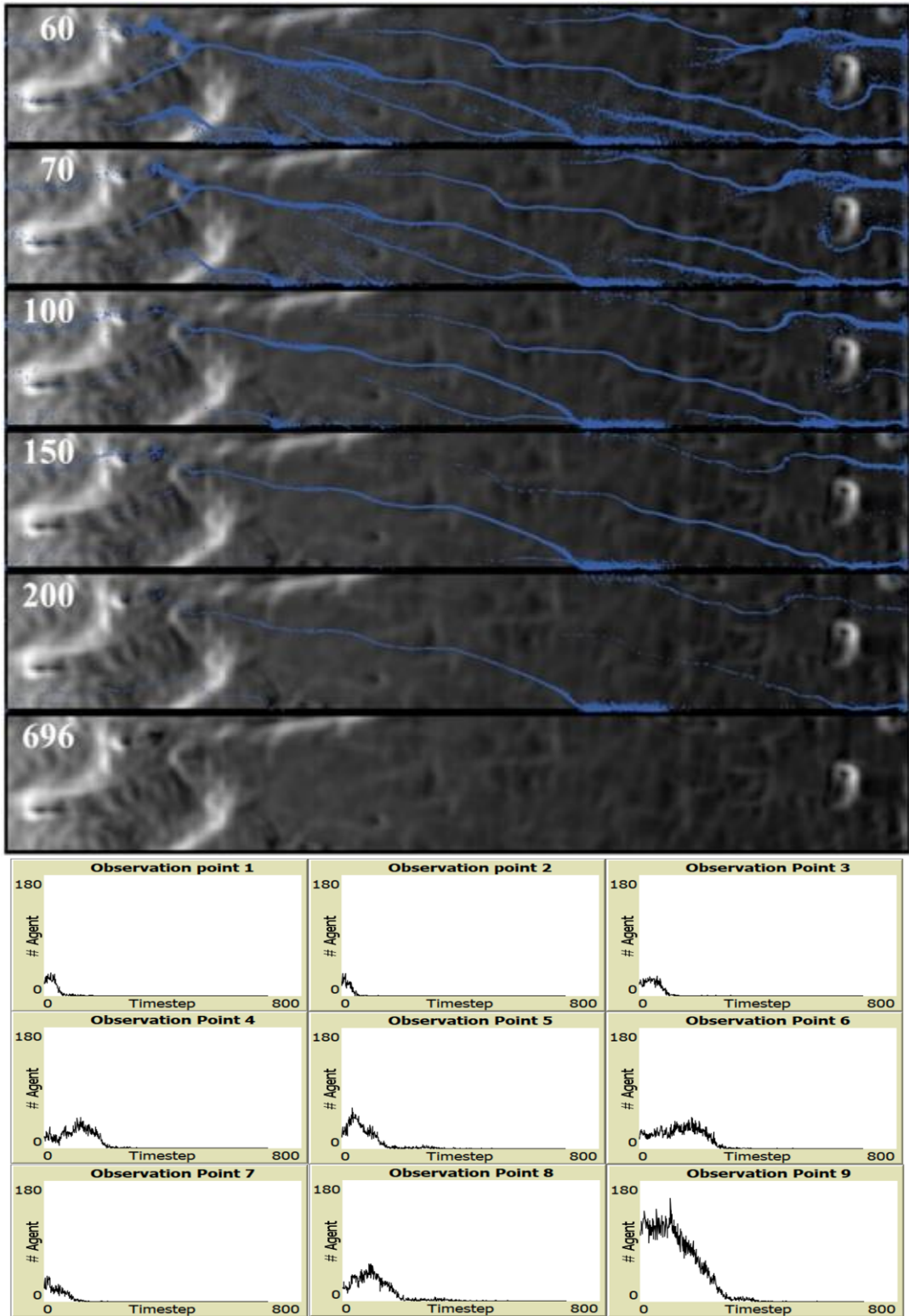


Fig. 5. Agent Based Modeling at timestep 60-696 (above) and Hydrograph at observation points (Below).

Meanwhile, the edifice of the Sinabung stratovolcano is formed only by one geological formation, producing a more perfect topography of the volcanic cone, which is efficient for a radial drainage pattern (i.e., shorter river channels with less meandering). As a consequence, the flow velocity is more rapid on the Sinabung volcano, with an average of 5.32 m/s compared to 4.12 m/s on the Merapi volcano. This faster flow velocity did not provide enough opportunity to form many pulsations.

In general, lahar histogram contains three main parts: lahar front, body and tail. These three main parts are also found in the model in this study through histogram (**Fig. 5**) and spatio-temporal distribution map of involved agents (**Fig. 4**). Each tributaries have flow front, body, and tail. Flow front is indicated by rapid augmentation of accumulated agent. Body is characterized by steady accumulation of agent, while tail is gradual diminution of the accumulated agent. Indeed, runoff at Sinabung volcano would erode pyroclastic materials that could trigger lahars (Nakada et al., 2019). The result of these lahars is abundant progressive aggradation that can be found along the Lau Borus River (Adriani and Nurwihastuti, 2017; Kadavi et al., 2017; Supriyati and Tjahjono, 2018).

Agent Based Model (ABM) used in this study is identic to Smoothed-Particle Hydrodynamics (SPH) which is defined as computational method to analyze two phase non-newtonian fluid (Albano et al., 2016; Hårdi et al., 2021). However, coupling between ABM and GIS allows us to retain geographic aspect within the model, such as DEM, slope, aspect, coordinates, and map algebra. This is important to help us bringing the real environment into the model where agents are set to react based on its behavior. The output of this model is adequate for flow analysis since it produced spatio-temporal map and also hydrogram.

5. CONCLUSIONS

This study emphasizes the development model of runoff flowing into the newly formed lake at Sinabung volcano. Its ongoing escalated volcanic activity and continuous eruption have been observed since 2010, although there has been no historical eruption of this volcano since 1600. Abundant pyroclastic materials from Sinabung volcano are eroded and deposited on the eastern and southern flanks, leading to the formation of a new lake at the Lau Borus River. A coupling between an Agent-Based Model and Geographic Information System is designed to conduct a dynamic model of runoff and spatio-temporal mapping.

Hydrographs from observation points allow for a comparison of flow dynamics between the two most active stratovolcanoes in the same tropical region (Sinabung and Merapi volcano). They share similar characteristics, such as runoff accumulation in the river channel that triggers lahars. However, they also exhibit two different characteristics regarding the quantity of flow pulsations due to their differences in the complexity of geological formations, topography, and drainage patterns. After identifying the accumulation process of runoff flowing into the newly formed lake at Sinabung volcano, further studies might be needed to anticipate the outburst of this new lake.

ACKNOWLEDGEMENT

This research was undertaken at the GIS Laboratory, Department of GIScience, Faculty of Geography, Universitas Gadjah Mada, as part of independent lecturer research. Badan Informasi Geospasial (BIG) and European Space Agency (ESA) were very helpful by granting easy access to DEM Data and Sentinel 2 imagery. We also express our gratitude to the anonymous reviewers and the editors for generously dedicating their time to offer constructive feedback.

REFERENCES

- Abebe, Y.A., Ghorbani, A., Nikolic, I., Vojinovic, Z., Sanchez, A. (2019) Flood risk management in Sint Maarten – A coupled agent-based and flood modelling method. *Journal of Environmental Management*, 248, 109317. <https://doi.org/10.1016/j.jenvman.2019.109317>
- Aerts, J.C.J.H. (2020) Integrating agent-based approaches with flood risk models: A review and perspective. *Water Security*, 11, 100076. <https://doi.org/10.1016/j.wasec.2020.100076>
- Albano, R., Sole, A., Mirauda D., Adamowski, J. (2016) Modelling large floating bodies in urban area flash-floods via a Smoothed Particle Hydrodynamics model. *Journal of Hydrology*, 541, Part A, 344-358. <https://doi.org/10.1016/j.jhydrol.2016.02.009>
- Aldriani, S., & Nurwihastuti D.W. (2017) Kajian Morfologi Sungai Lau Borus Di Kabupaten Karo Akibat Aliran Lahar Dingin Pasca Erupsi Gunungapi Sinabung Tahun 2016. *Tunas Geografi*. 6 (1), 74-87. <https://doi.org/10.24114/tgeo.v6i1.8351>
- Badan Informasi Geospasial, 2018. DEMNAS: Seamless Seamless Digital Elevation Model (DEM) dan Batimetri Nasional. Last access on 18 May 2023, <https://tanahair.indonesia.go.id/demnas/#/>.
- Carr, B.B., Clarke, A.B., Ramón Arrowsmith, J., Vanderkluisen, L., & Dhanu, B.E. (2019) The emplacement of the active lava flow at Sinabung Volcano, Sumatra, Indonesia, documented by structure-from-motion photogrammetry. *Journal of Volcanology and Geothermal Research*, 382, 164-172. <https://doi.org/10.1016/j.jvolgeores.2018.02.004>
- Chesner C.A., Barbee O.A., McIntosh W.C. (2020) The enigmatic origin and emplacement of the Samosir Island lava domes, Toba Caldera, Sumatra, Indonesia. *Bulletin of Volcanology*. 82, 26. <https://doi.org/10.1007/s00445-020-1359-9>
- Gomez C., Hotta H., Shinohara Y., Park J.-H., Tsunetaka H., Zhang M., Bradak B., Hadmoko D.S., Wibowo S.B., Daikai R., Yoshida M. (2023) Formation Processes of Gully-side Debris-Cones Determined from Ground-Penetrating Radar (Mt. Unzen, Japan). *Journal of Applied Geophysics*. 209, 104919. <https://doi.org/10.1016/j.jappgeo.2022.104919>
- Haer, T., Husby, T.G., Wouter Botzen, W.J., & Aerts, J.C.J.H. (2020) The safe development paradox: An agent-based model for flood risk under climate change in the European Union. *Global Environmental Change*, 60, 102009. <https://doi.org/10.1016/j.gloenvcha.2019.102009>
- Härdi, S., Schreiner, M., Janoske, U. (2021) On a new algorithm for incorporating the contact angle forces in a simulation using the shallow water equation and smoothed particle hydrodynamics. *Computers & Fluids*, 215, 104793. <https://doi.org/10.1016/j.compfluid.2020.104793>
- Hotta, K., Iguchi, M., Ohkura, T., Hendrasto, M., Gunawan, H., Rosadi, U., & Kriswati E. (2019) Magma intrusion and effusion at Sinabung volcano, Indonesia, from 2013 to 2016, as revealed by continuous GPS observation. *Journal of Volcanology and Geothermal Research*, 382, 173-183. <https://doi.org/10.1016/j.jvolgeores.2017.12.015>
- Indrastuti, N., Nugraha, A.D., McCausland, W.A., Hendrasto, M., Gunawan, H., Kusnandar, R., Kasbani, & Kristianto. (2019) 3-D Seismic Tomographic study of Sinabung Volcano, Northern Sumatra, Indonesia, during the inter-eruptive period October 2010–July 2013. *Journal of Volcanology and Geothermal Research*, 382, 197-209. <https://doi.org/10.1016/j.jvolgeores.2019.03.001>
- Kadavi, P., Lee, W.-J., & Lee, C.-W. (2017) Analysis of the Pyroclastic Flow Deposits of Mount Sinabung and Merapi Using Landsat Imagery and the Artificial Neural Networks Approach. *Applied Sciences*, 7(9), 935. doi:10.3390/app7090935
- Kriswati, E., Meilano, I., Iguchi, M., Abidin, H.Z., & Surono. (2019) An evaluation of the possibility of tectonic triggering of the Sinabung eruption. *Journal of Volcanology and Geothermal Research*, 382, 224-232. <https://doi.org/10.1016/j.jvolgeores.2018.04.031>
- Mukhopadhyay S., Roy B., Sangode S.J., Jaiswal M.K., Dutta S. (2022) Late Quaternary sediments from Barakar-Damodar Basin, Eastern India include the 74 ka Toba ash and a 17 ka microlith toolkit. *Journal of Asian Earth Sciences: X*. 9: 100135. <https://doi.org/10.1016/j.jaesx.2022.100135>
- Naen G.N.R.B., Toramaru A., Juhri S., Yonezu K., Wibowo H.E., Gunawan R.M.P.P., Disando T. (2023) Distinct pumice populations in the 74 ka Youngest Toba Tuff: Evidence for eruptions from multiple magma chambers. *Journal of Volcanology and Geothermal Research*. 437, 107804. <https://doi.org/10.1016/j.jvolgeores.2023.107804>

- Nakada, S., Zaennudin, A., Yoshimoto, M., Maeno, F., Suzuki, Y., Hokanishi, N., Sasaki, H., Iguchi, M., Ohkura, T., Gunawan, H., & Triastuty H. (2019) Growth process of the lava dome/flow complex at Sinabung Volcano during 2013–2016. *Journal of Volcanology and Geothermal Research*, 382, 120-136. <https://doi.org/10.1016/j.jvolgeores.2017.06.012>
- Ruan, H., Chen, H., Wang, T., Chen, J., & Li, H. (2021) Modeling Flood Peak Discharge Caused by Overtopping Failure of a Landslide Dam. *Water*, 13(7), 921. doi:10.3390/w13070921
- Sun, W., Zhang, Ga., Zhang, Z. (2021) Damage analysis of the cut-off wall in a landslide dam based on centrifuge and numerical modeling. *Computers and Geotechnics*, 130, 103936. <https://doi.org/10.1016/j.compgeo.2020.103936>
- Supriyati, & Tjahjono, B. (2018) Analisis Morfometri Bentanglahan Untuk Prediksi Bahaya Aliran Lahar Gunungapi Sinabung. *Seminar Nasional Geomatika 2018*. 1265-1272. <http://dx.doi.org/10.24895/SNG.2018.3-0.1052>
- Takayama, S., Fujimoto, M., Satofuka, Y. (2021) Amplification of flood discharge caused by the cascading failure of landslide dams. *International Journal of Sediment Research*, 36 (3), 430-438. <https://doi.org/10.1016/j.ijsrc.2020.10.007>
- Tsai, Y.-J., Syu, F.-T., Shieh, C.-L., Chung, C.-R., Lin, S.-S., & Yin, H.-Y. (2021) Framework of Emergency Response System for Potential Large-Scale Landslide in Taiwan. *Water*, 13(5), 712. doi:10.3390/w13050712
- Ville A., Lavigne F., Virmoux C., Brunstein D., De Bélizal E., Wibowo S. B., Hadmoko D. S. (2015) Geomorphological evolution of the Gendol valley following the October 2010 eruption of Mt Merapi (Java, Indonesia). *Geomorphology: relief, processus, environnement*, 21 (3), 235-250. <https://dx.doi.org/10.4000/geomorphologie.11073>
- Wibowo, S.B. (2010) Utilisation des classifications d'Oldeman et de Schmidt-Ferguson pour l'aptitude culturale des sols à Batu, Indonésie. In S. Khan, H.G.H Savenije, S. Demuth, P. Hubert (dir.). *Hydrocomplexity: new tools for solving wicked water problems*. IAHS publication, 338, 181-182
- Wibowo, S.B., Lavigne, F., Mourot, P., Métaixian, J.-P., Zeghdoudi, M., Virmoux, C., Sukatja, C.B, Hadmoko, D.S., Mutaqin, B.W. (2015) Coupling between Video and Seismic Data Analysis for the Study of Lahar Dynamics at Merapi Volcano, Indonesia. *Géomorphologie : relief, processus, environnement*. 21, 3, 251-266. doi: 10.4000/geomorphologie.11090
- Wibowo S.B., Nurani I.W. (2019) Improving geoinformation technology by incorporating local participation. *Proceedings of SPIE - The International Society for Optical Engineering*. 11311,113110C. <https://doi.org/10.1117/12.2550320>
- Wibowo S.B., Hadmoko D.S., Isnaeni Y., Farda N.M., Putri A.F.S., Nurani I.W., Supangkat S.H. (2021) Spatio Temporal Distribution of Ground Deformation Due to 2018 Lombok Earthquake Series. *Remote Sensing*. 13, 2222. <https://doi.org/10.3390/rs13112222>
- Yang, Q., Guan, M., Peng, Y., Chen, H. (2020) Numerical investigation of flash flood dynamics due to cascading failures of natural landslide dams. *Engineering Geology*, 276, 105765. <https://doi.org/10.1016/j.enggeo.2020.105765>
- Zhong, Q., Wang, L., Chen, S., Chen, Z., Shan Y., Zhang Q., Ren Q., Mei S., Jiang J., Hu, L., & Liu, J. (2021) Breaches of embankment and landslide dams - State of the art review. *Earth-Science Reviews*, 216, 103597. <https://doi.org/10.1016/j.earscirev.2021.103597>
- Zhong, Q., Chen, S., Shan, Y. (2020) Prediction of the overtopping-induced breach process of the landslide dam, *Engineering Geology*, 274, 105709. <https://doi.org/10.1016/j.enggeo.2020.105709>
- Zhuo, L., Han, D. (2020) Agent-based modelling and flood risk management: A compendious literature review. *Journal of Hydrology*, 591, 125600. <https://doi.org/10.1016/j.jhydrol.2020.125600>